EPJ Web of Conferences **10**, 00015 (2010)
DOI: 10.1051/epjconf/20101000015

Characterization of lithium fluoride windows at 450 K for shock wave experiments: Hugoniot curves and refractive index at 532 nm

E. Fraizier[a], P. Antoine, J.-L. Godefroit, G. Lanier, G. Roy, and C. Voltz

CEA Valduc, 21120 Is sur Tille, France

Abstract. Lithium fluoride (LiF) windows are extensively used in traditional shock wave experiments because of their transparency beyond 100 GPa along [100] axis. A correct knowledge of the optical and mechanical properties of these windows is essential in order to analyze the experimental data and to determine the equation of state on a large variety of metals. This in mind, the windows supply is systematically characterized in order to determine the density, the thermal expansion and the crystalline orientation. Furthermore, an experimental campaign is conducted in order to characterize the windows properties under shock loading at 300 K and preheated conditions (450 K). This article describes the experiments, details the analysis and presents the results. Particle velocity measurements are carried out at the interface of a multiple windows stack using interferometer diagnostic (VISAR and IDL) at 532 nm wavelength. Shock velocity is calculated as a function of the time of flight through each window. The optical correction is calculated as the ratio of the apparent velocity gap and the particle velocity at the free surface. To go further, the Rankine-Hugoniot relations are applied to calculate the pressure and the density. Then, the results and uncertainties are presented and compared with literature data.

1 Challenges for the LiF characterization

Traditional shock wave experiments need windows to characterize a variety of materials. Lithium fluoride (LiF) is extensively used for that purpose because it remains optically transparent until more than 100 GPa. In order to analyse and simulate the experiments it is necessary to have a good knowledge of the optical and mechanical properties of these LiF windows. This in mind it is necessary to characterize our windows supply: density, crystalline orientation, acoustic velocity and dimensional measurements. Furthermore, a campaign is conducted in order to characterize the behaviour under dynamic loading in particular at 450 K which is the selected temperature level for some of our preheated experiments [1].

2 Experiments principle and campaign

Under classical impact configuration the optical diagnostics measure the velocities at the interfaces (Fig. 1).

First of all, the shock wave time of flight Δt_{LiF} is measured at the interface and at the free surface with the VISAR. Knowing the thickness e_{LiF} of the LiF window, the shock wave velocity U_S is

[a] e-mail: emmanuel.fraizier@cea.fr

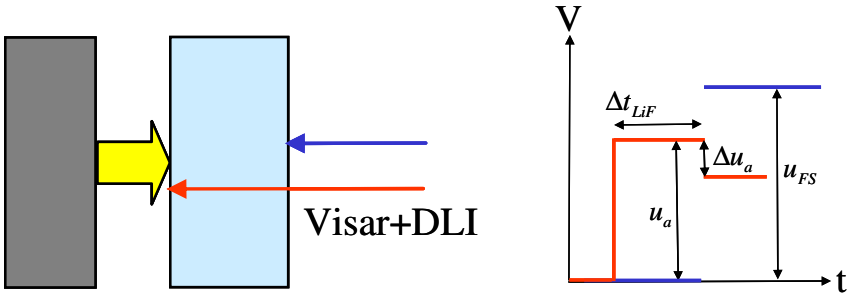

Fig. 1. Principle of the experiments and velocities diagnostics.

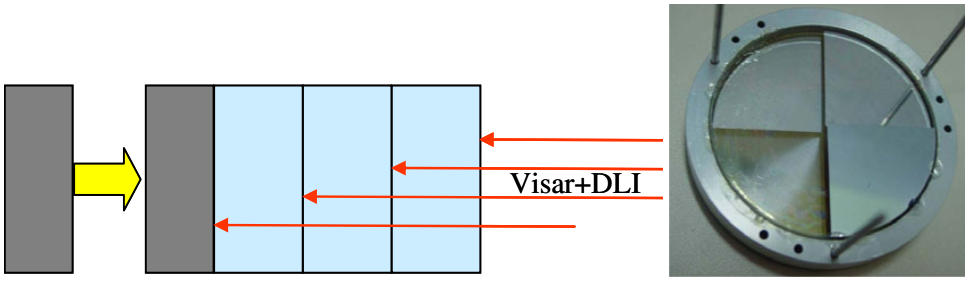

Fig. 2. Experimental assembly scheme and quarter coated windows.

calculated (1).

$$U_S = \frac{e_{LiF}}{\Delta t_{LiF}} \tag{1}$$

Secondly, relations from literature [2–7] allow to determine the optical corrective index $n_0 - \lambda$ from the ratio of the apparent velocity gap Δu_a (when the shock emerges at the free surface) and the velocity at the free surface u_{FS}.

$$k = n_0 - \lambda - 1 = \frac{\Delta u_a}{u_{FS}} \tag{2}$$

The actual particle velocity u_p at the interface is consequently determined (3).

$$u_p = \frac{u_a}{n_0 - \lambda} \tag{3}$$

To go further, the Rankine-Hugoniot relations are applied. The pressure is then calculated (4) and the shock density is expressed as a function of the initial density ρ_0, the shock velocity U_S and the particle velocity u_p (5).

$$P = \rho_0 U_S u_p \tag{4}$$

$$\rho = \rho_0 \frac{U_S}{U_S - u_p} \tag{5}$$

Finally, the refractive index n is determined as a function of density (6).

$$n = n_0 - \lambda + \lambda \frac{\rho}{\rho_0} \tag{6}$$

The experimental campaign is composed of two configurations using 3 mm thickness LiF windows (Fig. 2). The assembly is achieved with 3 glued samples at ambient temperature and 2 samples mechanically tied at 450 K. The windows are quarter coated (Fig. 1) to enable the velocity measurements

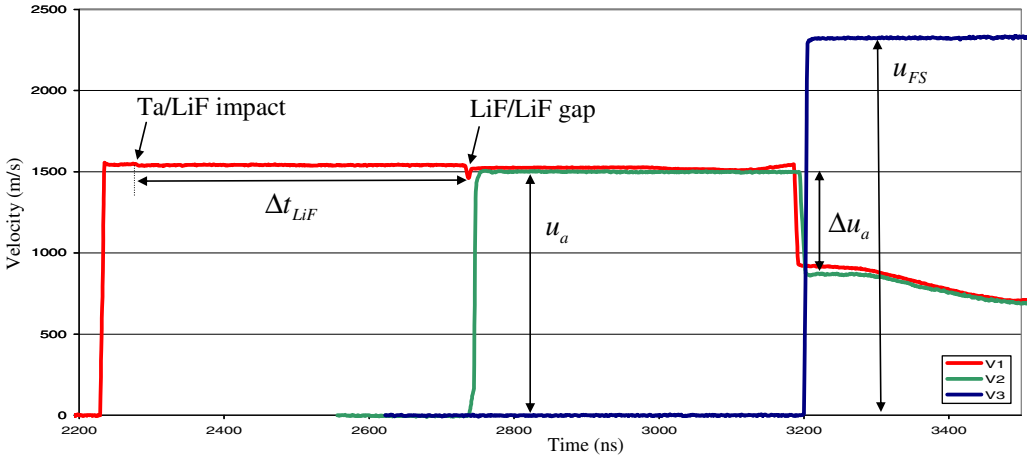

Fig. 3. VISAR diagnostic of the interfaces velocities.

at the different interfaces. The pressure ranges from 7 to 21 GPa using tantalum flyer and buffer. A computer simulation enables to predict the pressure and the velocity diagrams in order to adjust the optical diagnostics.

The LiF supplies (from BFI OPTILAS) are characterized to determine the following values:

- [100] for the crystalline orientation,
- 2.630 for the density at 300 K,
- $\alpha = 3.990 \times 10^{-11} \times T^2 + 5.125 \times 10^{-8} \times T + 3.225 \times 10^{-5}\,\mu\text{m.m}^{-1}.^{\circ}\text{C}^{-1}$ for the linear thermal expansion along the [100] axis [8].
- 6396 m.s^{-1} for the longitudinal acoustic velocity along the [100] axis.

The preheated system is calibrated on LiF apparatus with 6 temperature measurements. The homogeneity is less than 10 K on a window. Furthermore a computer thermal simulation (Fluent code) confirms these results.

3 Experiment analysis at 450 K and 20.4 GPa

This part presents the analysis of the VISAR results (Fig. 3) at the interfaces for the experiment conducted at 450 K and 20.4 GPa. The DLI measurements enable to check the apparent velocity using a second diagnostic.

Gaps in the assembly produce visible effects on velocity profiles. The velocity measured (without optical correction) on the tantalum buffer shows its free flight (46 ns) before the impact on the first LiF window. Furthermore, a local decrease of velocity corresponds to the gap between the two windows.

When the shock emerges at the free surface the classical velocity gap Δu_a is observed.

The first exploitation consists in the measurement of the shock time of flight Δt_{LiF} in the two windows. The shock velocity is calculated, knowing the thickness of both LiF windows. Then, the velocity plateau and the velocity gap when the shock emerged at the free surface are measured. Furthermore, the free surface velocity is also measured and the relation (2) is applied in order to determine the corrective index. At least, the Rankine-Hugoniot relations enable to calculate the shock pressure, density and refractive index (4–6).

Some values are directly measured from diagnostics giving their experimental uncertainties: it is the case for the windows thickness, the time of flight and the apparent velocities for examples. The other values are calculated from relations (1–6). In this case, two simple rules (7) and (8) are applied for

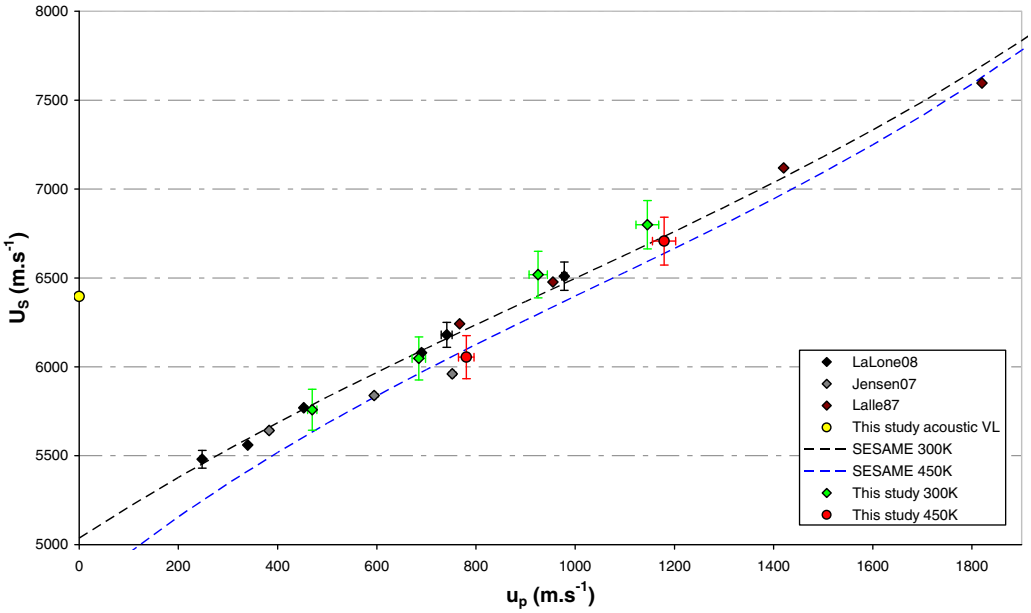

Fig. 4. Shock velocity as a function of the particle velocity.

the uncertainties calculation (and unfortunately their propagation). So, with experimental uncertainties of roughly 2% the calculated values reach more than 4–6% of uncertainties.

$$\frac{\Delta(a \times b)}{a \times b} = \frac{\Delta(a/b)}{a/b} = \frac{\Delta a}{a} + \frac{\Delta b}{b} \tag{7}$$

$$\Delta(a + b) = \Delta(a - b) = \Delta a + \Delta b \tag{8}$$

4 Experimental results

The Fig. 4 represents the shock velocity (1) as a function of the particle velocity (2–3). Our results are compared to the literature data at ambient temperature. They are in good agreement with the results from Lalone [9] and Lalle [6,7] but show strong deviation from Jensen data [10]. Furthermore, the SESAME data (dashed lines) are consistent with our uncertainty level at ambient temperature and at 450 K. The initial temperature dependence is evident and a decrease of the shock velocity is observed for the preheated experiments.

To go further, the pressure and density are calculated. The refractive index is then calculated from the relations (2) and (6). Furthermore, the density is normalised with the initial density $\rho_0\,(T)$ corresponding to the initial temperature of the experiment. Applying the measured linear expansion (along [100] axis), with the first approximation of an isotropic material, the calculated density at 450 K is 2.582. Once again our results are in better agreement with data from Lalone [9] than from Jensen [10]. As for them, a linear fit taking our uncertainties into account is achieved (9).

$$n = (1.2926 \pm 0.1263) + (0.1013 \pm 0.1090)\,\frac{\rho}{\rho_0} \tag{9}$$

These results serve some remarks to emphasize that the initial density is a crucial parameter to explain some shift on the ρ/ρ_0 axis. Indeed, the literature references use initial density at ambient temperature which are different from our 2.630 measurement: 2.641 [9,10] and 2.638 [6,7]. As a result, this observation could explain shifts of the linear fits and in particular of the optical index determination given for $\rho = \rho_0$.

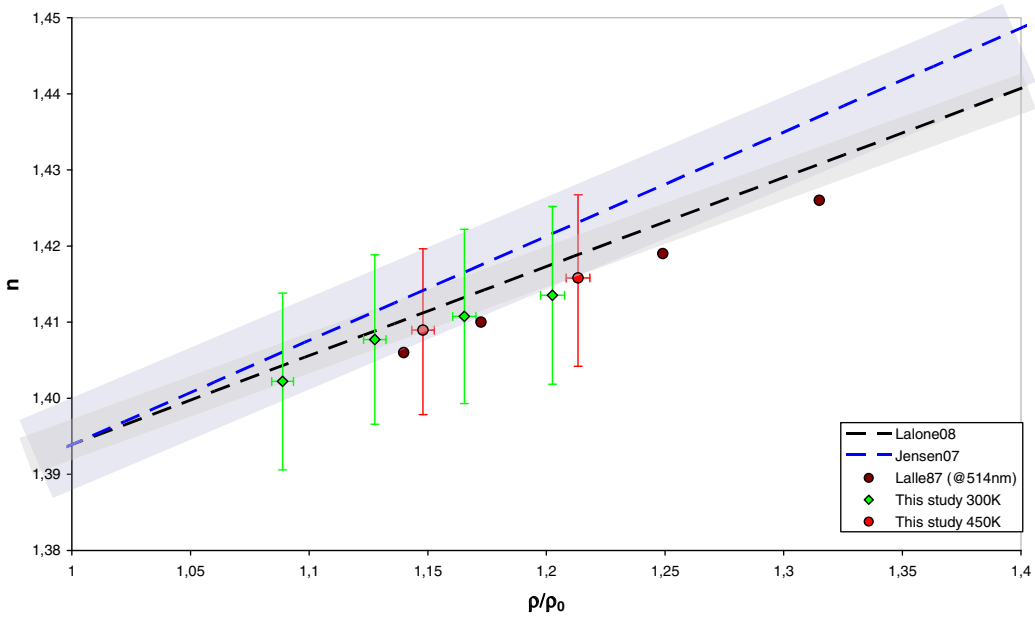

Fig. 5. Refractive index as a function of the normalized density.

Nevertheless, differences with the study of Lalle [6,7] realized at 514 nm are also explained because the refractive index is a function of wavelength.

Finally, a further study is necessary to measure directly the density as a function of temperature. Indeed, the LiF has a crystalline orientation and the application of the linear expansion (isotropic approximation) could be discussed and improved in future works.

5 Conclusions and future works

The present work is in good agreement with literature data at ambient temperature. Few differences could be explained by different supplies and initial density used. Furthermore, the optical and mechanical characterization conducted under shock at 450 K enables a better interpretation of our preheated experiments on a variety of materials.

Taking into account the initial temperature through the initial density, our results confirm the theory that the refractive index is a linear function of the normalized density ρ/ρ_0 and a 1.2926 ± 0.1263 corrective index is obtained. The preliminary characterization of the LiF windows is a key point and the initial density merits a particular attention.

So, a future work is planned to measure the windows density at the initial temperature of our experiments. Furthermore, the uncertainties need to be improved for a better interpretation of the experiments involving window. For that purpose, simplified target configurations seem to be a promising way. A new campaign should also be conducted for the shock and optical characterization of sapphire windows.

References

1. G. Roy and al, *BAGHEERA: A new experimental facility at CEA/Valduc for actinides studies under high dynamic loading*, J. Phys. IV France **134**, pp. 731-737, (2006).
2. L. Barker and R.E. Hollenbach, J. Appl. Phys. **41**, 4208, (1970).
3. E.U. Condon and H. Odishan, Handbook of Physics, pp. 6-109, (1958).

4. D.R. Goosman, J. Appl. Phys. **65**, (1989).
5. J. Wackerle, H.C. Stacy and J.C. Dallman, Pro. Inst. Soc. Opt. Eng (SPIE) **832**, 72 (1987).
6. P. Lalle, Internal report CEA, (1987).
7. P. Lalle, Internal report CEA, (1997).
8. O. Duret, Internal report CEA, (2009).
9. B.M. Lalone, O.V. Fat'yanov, J.R. Asay and Y.M. Gupta, *Velocity correction and refractive index changes for [100] lithium fluoride optical windows under shock compression, recompression, and unloading,* Journal of applied physics **103**, (2008).
10. B.J. Jensen, D.B. Holtkamp, P.A. Rigg, D.H. Dolan, *Accuracy limits and window corrections for photon Doppler velocimetry*, Journal of applied physics **101**, (2007).